10 Lecture, 5 October 1999

10.1 Aberration compensation for spherical primaries: the Schmidt camera

All-reflecting optical systems are called *catoptric*; all-refracting systems are called *dioptric*. Mixed systems thus are called *catadioptric.* Telescopes made in this latter style include the Schmidt and Bouwers-Maksutov "cameras," and boast the largest unblurred fields of view among large telescopes (exceeding 10° in the 1-2 m diameter class). The fields of view are large enough to outweigh for certain purposes the limitations of telescopes with refractive elements, and thus are worthy of our attention. All of these cameras involve clever use of the symmetry of spherical primary mirrors to avoid the off-axis aberrations, coma, astigmatism and distortion, by never introducing them in the first place, and their design is a straightforward problem of compensation of the mirror's spherical aberration. In the following we will analyze the spherical aberration of the spherical mirror in a Schmidt camera and prescribe its compensation with a refractive "corrector plate."

The crucial feature of Schmidt cameras is the presence of a circular entrance aperture placed with its center at the curvature center of a spherical mirror (Figure 10.1). For any ray bundle passing through this aperture, the chief ray passes through the center of the sphere, *and therefore is perpendicular to the sphere's surface*. In other words, all ray bundles passing through the entrance aperture are on axis, no matter what their angle with the perpendicular to that aperture. An image is therefore formed on the spherical focal surface halfway between the spherical mirror and its center, and the only aberration present is spherical aberration. Schmidt realized that he could compensate for the SA by placing a refracting corrector at the entrance aperture, and that the corrector would not reintroduce the other third-order aberrations on the same magnitude as those of a comparably-large conic-section mirror.

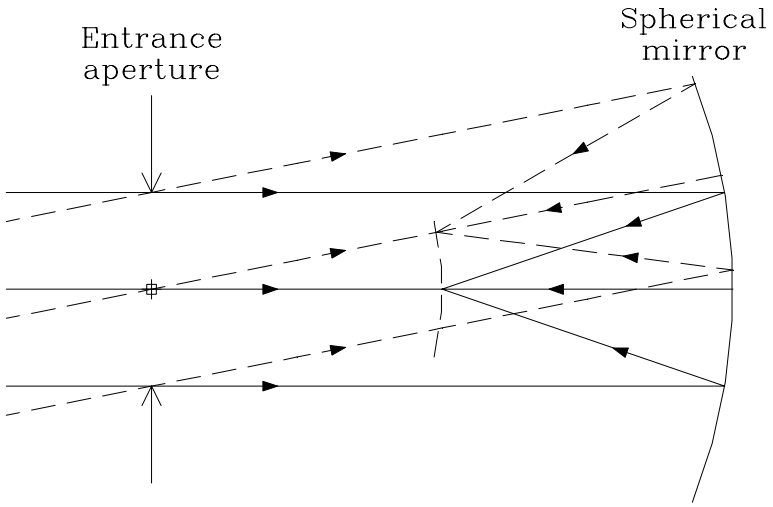

Figure 10.1: optical setup for the Schmidt camera. Both ray bundles are on axis, in the sense that the chief ray is perpendicular to the mirror surface and passes through its curvature center.

We can follow Schmidt's tracks by employing the angular-aberration and reference surface formalism used above. Consider the track of a ray incident a distance y from the axis, as in Figure 10.2, in a Schmidt camera with mirror curvature κ. This ray would normally reflect through a point which according to Equation 7.13 lies a distance $\Delta f = -\kappa y^2 / 4$ from the paraxial focus. A paraboloid with its apex on the

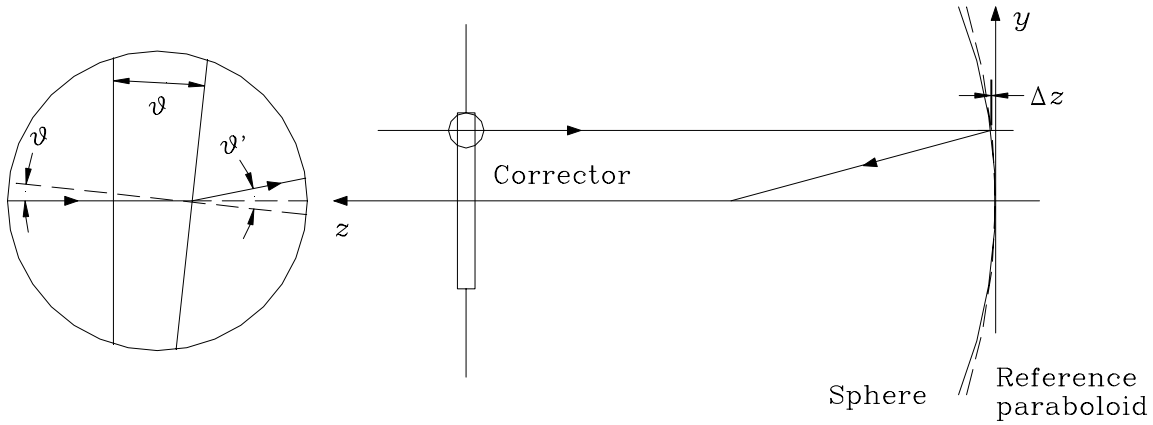

Figure 10.2: aberration compensation in the Schmidt camera.

sphere and focus on the sphere's paraxial focus is therefore the appropriate reference surface. The angular aberration of our ray is given as usual by $AA_0 = d(2\Delta z)/dy$, for which, according to Equation 7.10, we have the third order expression

$$AA_0 = \frac{d}{dy}(2\Delta z) = \frac{d}{dy}\left(-\frac{\kappa^3 y^4}{4}\right) \quad . \tag{10.1}$$

Now consider the action of a thin dielectric prism with opening angle θ placed in the entrance aperture in the path of this ray, with its front face perpendicular to the ray. With the orientation shown in Figure 10.2, the ray would be refracted away from the axis by an angle such that $\sin\theta' = n\sin\theta$, for a net angular deviation from its original direction of $AA_1 = \theta' - \theta$. The angle θ is simply related to the slope of the second prism surface, $\tan\theta = -dz_c/dy$, where z_c is the position of the oblique prism surface at point y, and where the minus sign comes from the leftward orientation of the z axis. If all of these angles are small we therefore have

$$AA_1 = (n-1)\theta = \frac{d}{dy}\left(-(n-1)z_c\right) \quad . \tag{10.2}$$

For cancellation of the angular aberrations, we can integrate the expression $AA_0 + AA_1 = 0$, and get

$$(n-1)z_c + \frac{\kappa^3 y^4}{4} = \text{constant} \quad ,$$

or

$$z_c = \frac{\kappa^3 y^4}{4(n-1)} + z_{c0} \quad , \tag{10.3}$$

where z_{c0} is a constant, for the reflection of all rays through the paraxial focus; spherical aberration is thus corrected to third order. This is a surface for which the slope is small at small y, so that paraxial rays suffer little deviation, but that provides large enough deviation for marginal rays to reach the same focus. It is illustrated in Figure 10.3.

The preceding is only the simplest and most obvious prescription for a Schmidt corrector. In practice somewhat smaller aberrations are obtained not by correcting all rays for the paraxial focus, but instead for

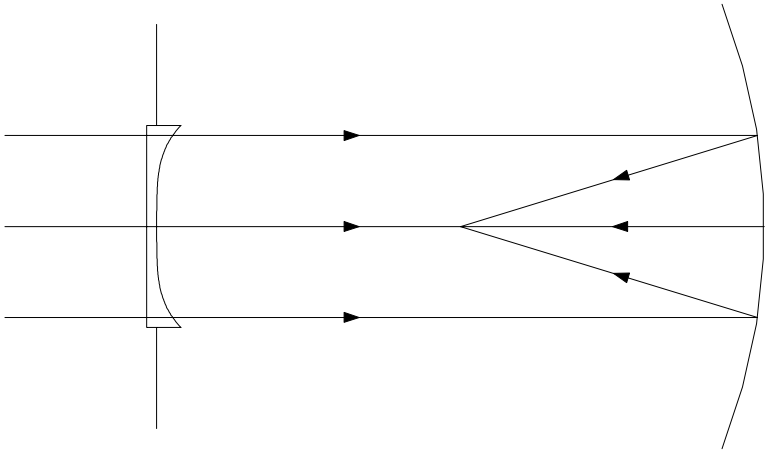

Figure 10.3: Schmidt camera with corrector prescribed by Equation 10.3. The coordinate system of Figure 10.2 applies, and the integration constant z_{c0} has been set equal to the sphere's radius. For clarity, the surface relief for the corrector's second surface has been drawn at a scale a factor of 100 larger than that used for the rest of the drawing.

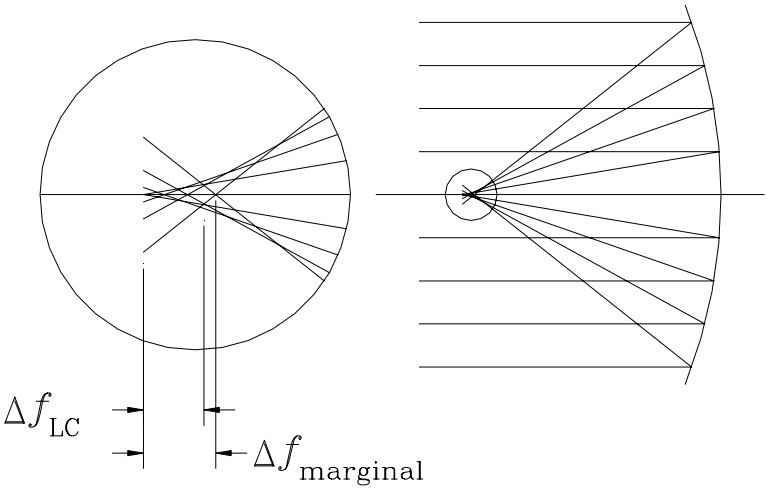

Figure 10.4: on-axis rays reflected from a spherical mirror, viewed near the focus. Distances are indicated from the paraxial focus to the circle of least confusion (LC) and the marginal-ray focus.

a focus at the position of the *circle of least confusion*. We have seen the circle of least confusion before, in computer ray-traces of spherical surface systems; for instance in problem 6 on Homework Problem Set #2, in which a spherical-mirror telescope with the same paraxial parameters as a classical Cassegrain and a Ritchey-Chretien exhibits its smallest RMS image diameter slightly closer to the mirrors than the other two telescopes. The position of the circle of least confusion can easily be estimated graphically, as in Figure 10.4. Calculations too detailed to include here indicate that this position actually lies three-quarters of the way from the paraxial focus to the marginal focus, in good agreement with Figure 10.4. With a glance at Equation 7.13 we see that the distance of this point from the paraxial focus is

$$\Delta f_{LC} = -\frac{3\kappa y_0^2}{16} \quad , \tag{10.4}$$

where y_0 is the off-center distance for marginal rays. There are of course on-axis rays that reflect through the axis in this position without a corrector; the corresponding off-center distance y' for these rays is given by Equation 7.13 again,

$$\Delta f = -\frac{\kappa y'^2}{4} = \Delta f_{LC} = -\frac{3\kappa y_0^2}{16} \quad , \tag{10.5}$$

or

$$y' = \frac{\sqrt{3}}{2} y_0 = 0.866 y_0 \quad . \tag{10.6}$$

To design a corrector for a focus at the circle of least confusion the appropriate reference mirror surface needs to have its focus there; if we choose a reference paraboloid with its apex on the spherical mirror it will have an apex curvature κ' different from the sphere's curvature, and given by

$$\frac{1}{2\kappa'} - \frac{1}{2\kappa} = \Delta f_{LC} = -\frac{3\kappa y_0^2}{16} \quad , \tag{10.7}$$

or

$$\kappa' = \frac{\kappa}{1 - \frac{3\kappa^2 y_0^2}{8}} \cong \kappa\left(1 + \frac{3\kappa^2 y_0^2}{8}\right) \quad . \tag{10.8}$$

Now the surface displacement between reference and sphere is

$$\begin{aligned} \Delta z &= \frac{\kappa' y^2}{2} - \frac{\kappa y^2}{2} - \frac{\kappa^3 y^4}{8} \\ &= \frac{3\kappa^3 y_0^2 y^2}{16} - \frac{\kappa^3 y^4}{8} \quad , \end{aligned} \tag{10.9}$$

and Equation 10.3 for the condition of cancellation of angular aberrations becomes

$$(n-1) z_c - \frac{3\kappa^3 y_0^2 y^2}{8} + \frac{\kappa^3 y^4}{4} = \text{constant} \quad ,$$

or

$$z_c = \frac{3\kappa^3 y_0^2 y^2}{8(n-1)} - \frac{\kappa^3 y^4}{4(n-1)} + z_{c0} \quad . \tag{10.10}$$

This result is depicted schematically in Figure 10.6, and compared to the result of Equation 10.3 in Figure 10.6. It gives rise to a corrector thickest at the center and thinnest at radius $y' = y_0\sqrt{3}/2$, that deviates all rays except those incident on these thickest and thinnest spots.

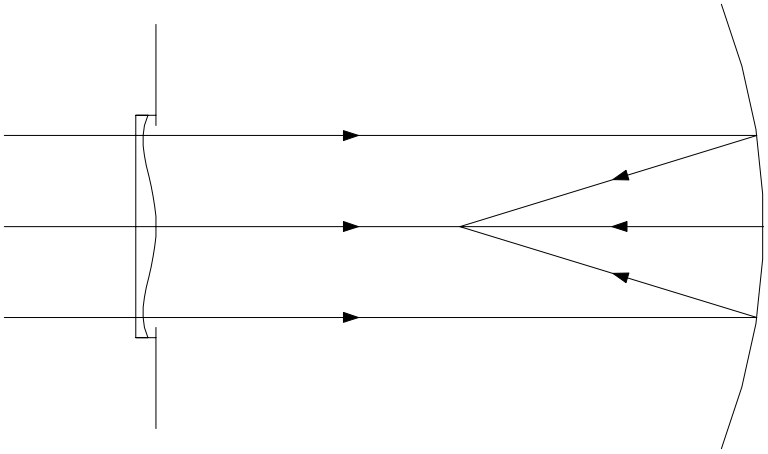

Figure 10.5: Schmidt camera with corrector prescribed by Equation 10.10. As in Figure 10.3, the integration constant z_{c0} has ben set equal to the sphere's radius, and the surface relief for the corrector's second surface has been drawn at a scale a factor of 100 larger than that used for the rest of the drawing, and the apex of the figured surface lies at the sphere's center.

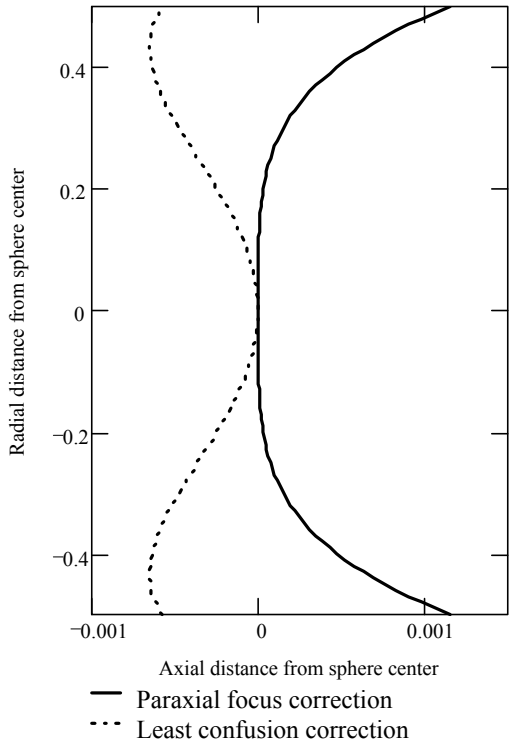

Figure 10.6: cross section of the Schmidt corrector surfaces given by Equation 11.3 (solid curve) and Equation 11.10 (broken curve), for $z_{c0} = 1/\kappa$ and for focus of all rays respectively to the paraxial focus and the circle of least confusion, for cameras with primary mirror radius a factor of three larger than the entrance aperture diameter. Both axes are plotted in units of the aperture diameter; note the differences of scale. The apex of each figure is placed at the center the sphere.

Now, some coma, astigmatism and distortion are introduced by either corrector, because although any ray bundle whose chief ray passes through the sphere's center is on axis for the sphere, only the one perpendicular to the entrance aperture is on axis for the corrector. These distortions are small compared to those introduced by a conic-section mirror of the same diameter. However, it is interesting to note that it is possible to cancel SA with a spherically-symmetric corrector. During the 1940s Bouwers and Maksutov independently noticed that a dielectric with two spherical surfaces that are concentric with the spherical mirror (and to which therefore all ray bundles are on axis) displaces, rather than deviates, off-center rays outward by an amount steeply dependent on off-center distance. This of course is the direction such rays would have to be placed in order to be reflected through the paraxial focus. Bouwers and Maksutov showed that by judicious choice of the corrector index and curvatures this scheme could be used to cancel spherical aberration; coma, astigmatism and distortion are also obviously absent. The only distortion remaining is Petzval field curvature; here manifest as the still-spherical focal surface.

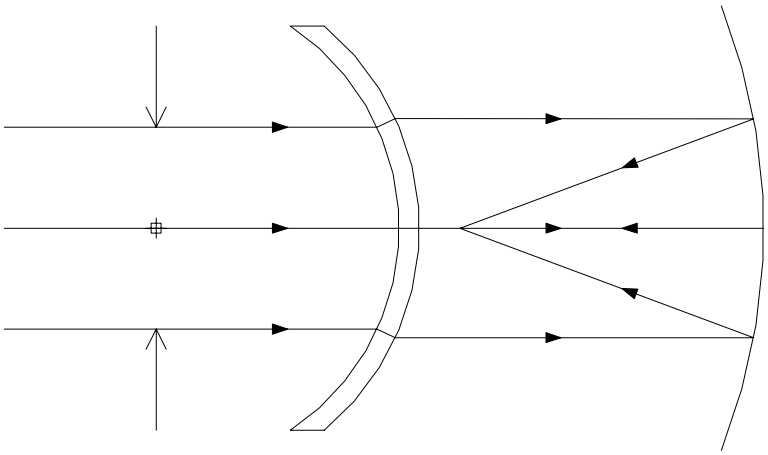

Figure 10.7: Bouwers-Maksutov camera, with all spherical surfaces concentric and with corrector index and radii chosen to eliminate third-order SA. The outward displacement of the marginal rays has been exaggerated greatly for clarity.

10.2 Large-diameter spherical primaries with multiple-element correctors

Spherical mirrors are easier to fabricate and test than the other conics. Because "easier" often means "less expensive," spherical primary mirrors are sometimes considered even when designers are not particularly interested in having a large field of view. Prime examples are the 305 m diameter Arecibo radio telescope in Puerto Rico, and more recently, the 10 m Hobby-Eberly Telescope (HET) in west Texas (Figure 10.8). In these cases the designers chose spherical primaries to enable tracking of celestial objects essentially by moving the detectors around near the prime focus, instead of by moving the whole mirror and telescope assembly. This would enable a huge cost savings for telescopes in these sizes. That this is possible is illustrated in Figure 10.9 (or, for that matter, in Figure 10.1). Only a fraction of the fixed-position primary mirror is used at any given time, and this fraction determines the maximum length of time that a celestial object may be tracked – the smaller the fraction, the longer the tracking time.

The HET mirror is hexagonal in projection, and is made up of 91 hexagonal mirror segments. This is another area in which the HET designers took advantage of the spherical geometry: these 91 segments are identical, and all spheres themselves, so to the extent that they can be mass-produced an economy of scale can be achieved. The 36 segments in each primary mirror of the Keck Telescopes, on the other hand, are all off-axis hyperboloids, with curvature that depends upon a segment's position in the primary-mirror mosaic

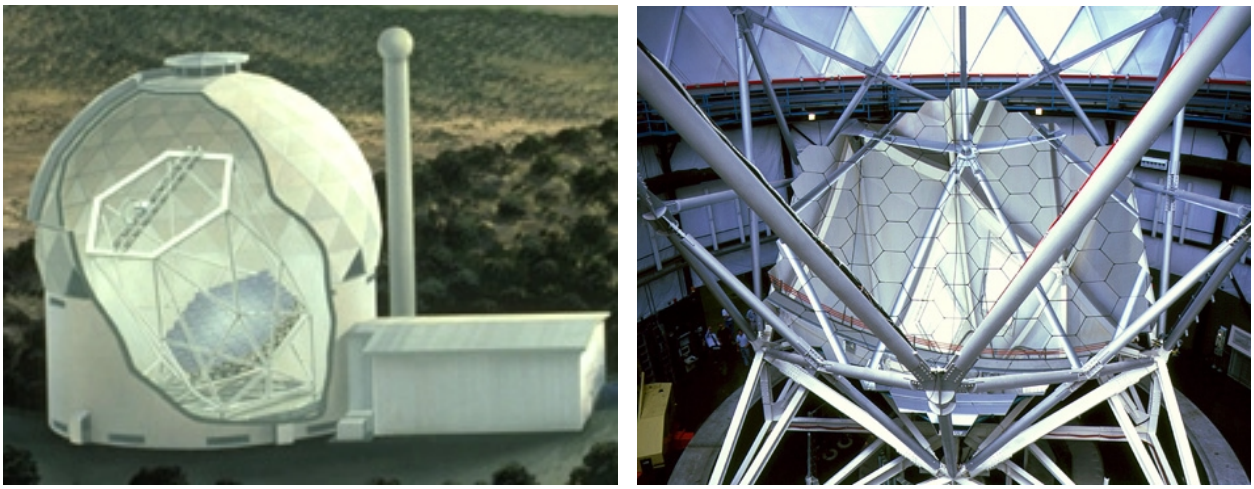

Figure 10.8: the Hobby-Eberly Telescope. *Left*: artist's rendition of telescope within dome. *Right:* photograph of the completed, spherical primary mirror.

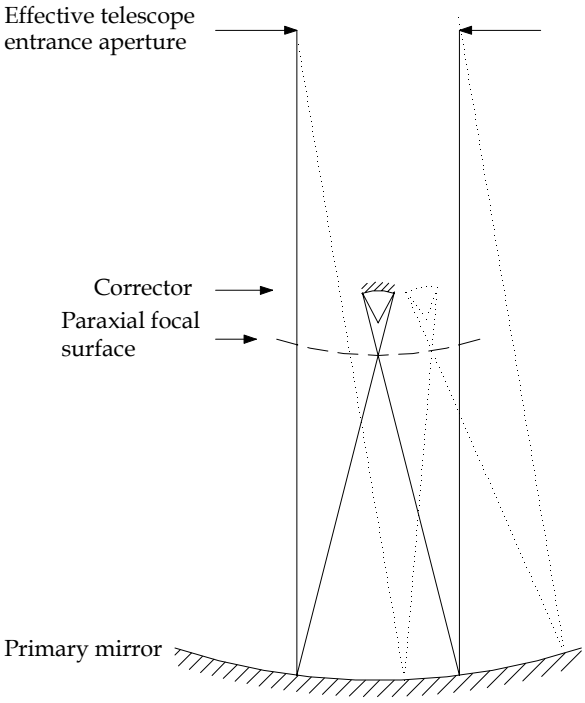

Figure 10.9: spherical-primary telescope with single-element Gregorian corrector. The position of corrector and marginal rays is shown for two different pointings of the telescope, in solid or dotted lines.

As one might imagine from the size of such primary mirrors, the spherical aberration is truly huge, and its correction is quite a challenging optical design project. When the Arecibo telescope was first built, the fact that a single detector was used in its focal plane (rather than an imaging detector array) was put to use in the solution of the spherical aberration problem with a *line feed.* Note that meridional rays from a point source, incident on opposite sides of the mirror, intersect along the radius of the sphere that points back to the point source, and that these intersection points are distributed along a segment of length Δf ,

given to fifth order by Equation 7.13. The line feed is a slotted linear waveguide, $\ell = -\Delta f$ in length, designed to pick up the light along this linear image and conduct it to the detector in the proper phase:

$$\ell = -\Delta f = \frac{\left(1-\varepsilon^2\right)\kappa y^2}{4} + \frac{\left(3-\varepsilon^2\right)\left(1-\varepsilon^2\right)\kappa^3 y^4}{16} \quad . \tag{10.11}$$

The relevant dimensions of Arecibo are $y = 152.4$ m, $1/\kappa = 265.18$ m, and $\varepsilon = 0$, which gives $\ell = 27.32$ m (!) for a feed that receives light from the entire telescope primary *. Originally the telescope was used with a line feed 12.19 m long, that received light from a 213.36 m diameter portion of the primary. This enabled celestial objects to be tracked up to about 11° from the primary mirror's axis without any of the detector's field of view spilling off the primary, and up to about 20° without losing more than half the signal.

Homework problem 10.1: An Arecibo-like telescope has a primary mirror with curvature radius *r* and diameter *D*, and a detector that can see a circular portion of the primary with diameter *d*. Show that the detector can view celestial objects within an angle

$$\theta = \arcsin\frac{D}{2r} - \arcsin\frac{d}{2r} \tag{10.12}$$

of the primary mirror's axis, without any of the detector's field of view missing the primary mirror.

Suppose that a telescope the same size as Arecibo is built on the Earth's equator, and is used to observe an object lying on the celestial equator. If one wishes not to let the detector's view spill off the primary mirror, what is the maximum length of time that this object can be observed?

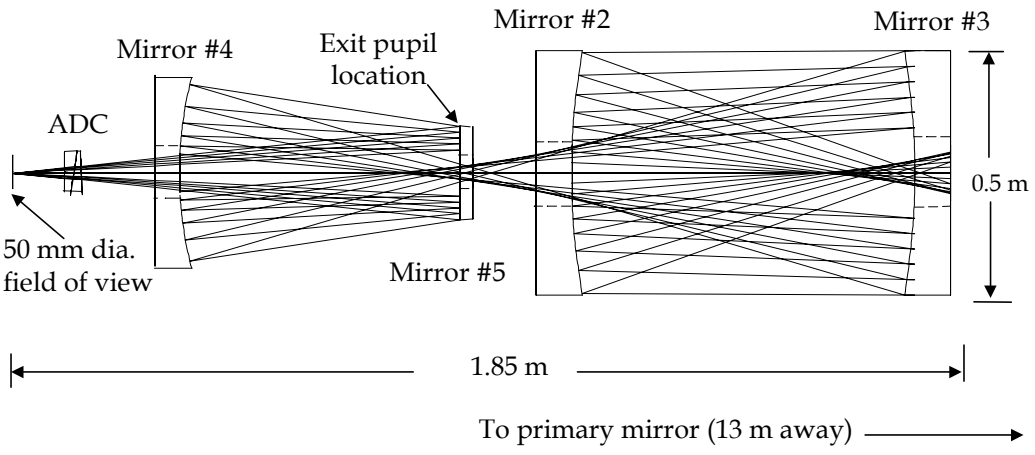

Figure 10.10: schematic diagram of the four-mirror corrector of the Hobby-Eberly Telescope (L. Ramsay, Penn. State University).

* This result is a bit short, because SA of order higher than fifth has become significant. The line feed that can receive light from the entire primary mirror is actually 29.5 m long, to account for higher-order SA.

Nowadays, reflective Gregorian style correctors are employed on both the Arecibo and Hobby-Eberly telescopes. To achieve adequate image quality it winds up being necessary to use several mirrors each telescopes corrector: two in the case of Arecibo, and four in the case of the Hobby-Eberly telescope. The latter is illustrated in Figure 10.10. An impression of the steps required for such SA correction can be gained in simpler fashion in homework problem 10.2.

Homework problem 10.2: *A single-element Gregorian spherical-aberration corrector.* You will do three ray traces in this problem; make sure they're all done with the same number of rays.

a. Consider a 200 cm diameter, spherical mirror with focal length 400 cm and a 40 cm, circular hole in the center. (The role of the hole will be made clear below.) Use RayTrace, with parallel on-axis rays (far field, DX=DY=0), to plot a spot diagram and to compute the RMS spot size at the position of best focus. Calculate the plate scale for the mirror, and use this to find the angular spread on the sky corresponding to this blur.

b. Next, consider a 200 cm diameter *paraboloid* mirror with the same focal length and central-hole size as the sphere in part a. Use with this an ellipsoidal secondary mirror, 40 cm in diameter, with on-axis focal lengths 80 cm and 40 cm, but instead of using the usual Gregorian arrangement, place the *far* focus in coincidence with the paraboloid's focus, so that the final image is formed closer to the ellipsoid's apex than the prime-focus image, as shown in Figure 10.9. Calculate the apex radius of curvature and eccentricity this mirror must have, and the plate scale at the final focus. Now use RayTrace and on-axis rays to plot a spot diagram and to compute the RMS spot size at the position of best focus, and calculate angular size on the sky corresponding to this blur.

c. Now, bend the mirrors in the telescope from part b: leave the apex curvatures and distances fixed, but change the eccentricity of the primary to zero (thus transforming it into the spherical mirror of part a), and calculate the eccentricity the secondary must have in order that third-order spherical aberration is corrected. Use these new eccentricities in RayTrace to plot a spot diagram and compute an RMS spot size. Calculate the angular size on the sky corresponding to this blur.

d. By what factor has the blur decreased from part a to part c? Account for the secondary's magnification in your answer.

e. Why isn't the blur in the telescope of part c as small as that of the telescope in part b?

